Journal of Ginseng Research 46 (2022) 550–560

Contents lists available at ScienceDirect

Journal of Ginseng Research

journal homepage: https://www.sciencedirect.com/journal/journal-of-ginseng-research

Research Article

Effects of G-Rh2 on mast cell-mediated anaphylaxis via AKT-Nrf2/NF-κB and MAPK-Nrf2/NF-κB pathways

Chang Xu [a, b, 1], Liangchang Li [a, b, 1], Chongyang Wang [a, b], Jingzhi Jiang [a, b], Li Li [a, b], Lianhua Zhu [b, c], Shan Jin [b, c], Zhehu Jin [b, c], Jung Joon Lee [e], Guanhao Li [a, d, **], Guanghai Yan [a, b, *]

[a] Jilin Key Laboratory for Immune and Targeting Research on Common Allergic Diseases, Yanbian University, Yanji, China
[b] Department of Anatomy, Histology and Embryology, Medical College, Yanbian University, Yanji, China
[c] Department of Dermatology, Yanbian University Hospital, Yanji, China
[d] Food Research Center of Yanbian University, Yanji, China
[e] College of Pharmacy, Yanbian University, Yanji, China

ARTICLE INFO

Article history:
Received 11 May 2020
Received in revised form
4 August 2021
Accepted 4 October 2021
Available online 13 October 2021

Keywords:
Ginsenoside Rh2 (G-Rh2)
AKT-Nrf2
MAPK-Nrf2
Mast cell

ABSTRACT

Background: The effect of ginsenoside Rh2 (G-Rh2) on mast cell-mediated anaphylaxis remains unclear. Herein, we investigated the effects of G-Rh2 on OVA-induced asthmatic mice and on mast cell-mediated anaphylaxis.

Methods: Asthma model was established for evaluating airway changes and ear allergy. RPMCs and RBL-2H3 were used for *in vitro* experiments. Calcium uptake, histamine release and degranulation were detected. ELISA and Western blot measured cytokine and protein levels, respectively.

Results: G-Rh2 inhibited OVA-induced airway remodeling, the production of TNF-α, IL-4, IL-8, IL-1β and the degranulation of mast cells of asthmatic mice. G-Rh2 inhibited the activation of Syk and Lyn in lung tissue of OVA-induced asthmatic mice. G-Rh2 inhibited serum IgE production in OVA induced asthmatic mice. Furthermore, G-Rh2 reduced the ear allergy in IgE-sensitized mice. G-Rh2 decreased the ear thickness. *In vitro* experiments G-Rh2 significantly reduced calcium uptake and inhibited histamine release and degranulation in RPMCs. In addition, G-Rh2 reduced the production of IL-1β, TNF-α, IL-8, and IL-4 in IgE-sensitized RBL-2H3 cells. Interestingly, G-Rh2 was involved in the FcεRI pathway activation of mast cells and the transduction of the Lyn/Syk signaling pathway. G-Rh2 inhibited PI3K activity in a dose-dependent manner. By blocking the antigen-induced phosphorylation of Lyn, Syk, LAT, PLCγ2, PI3K ERK1/2 and Raf-1 expression, G-Rh2 inhibited the NF-κB, AKT-Nrf2, and p38MAPK-Nrf2 pathways. However, G-Rh2 up-regulated Keap-1 expression. Meanwhile, G-Rh2 reduced the levels of p-AKT, p38MAPK and Nrf2 in RBL-2H3 sensitized IgE cells and inhibited NF-κB signaling pathway activation by activating the AKT-Nrf2 and p38MAPK-Nrf2 pathways.

Conclusion: G-Rh2 inhibits mast cell-induced allergic inflammation, which might be mediated by the AKT-Nrf2/NF-κB and p38MAPK-Nrf2/NF-κB signaling pathways.

1. Introduction

Type I hypersensitivity reaction, also known as anaphylaxis, usually occurs within minutes after the host is again exposed to the allergen [1]. Re-entry of the antigen induces mast cell degranulation to release inflammatory factors, thus causing allergic diseases such as asthma [2]. The main cause of asthma is contraction of smooth muscle caused by mast cell degranulation [3]. Mast cells degranulate and release histamine, resulting in contraction of pulmonary tracheal smooth muscles and causing dyspnea [4]. In

* Corresponding author. Department of Anatomy, Histology and Embryology, Medical College, Yanbian University, No. 977 Gongyuan Road, Yanji, 133002, PR China.
** Corresponding author. Food Research Center of Yanbian University, No. 977 Gongyuan Road, Yanji, 133002, PR China.
E-mail addresses: 1678233732@qq.com (G. Li), ghyan2015@sina.com (G. Yan).
[1] These authors contributed equally to this work.

https://doi.org/10.1016/j.jgr.2021.10.001

addition, mast cells release a large number of inflammatory cytokines such as IL-1β, TNF-α, IL-8, and IL-4 after sensitization [5,6]. Recent studies have shown that mast cell degranulation in asthma is mainly regulated by nuclear Ca^{2+} signal [7,8]. This entry of Ca^{2+} ions into the cell triggers the degranulation and secretion process. Therefore, inhibition of mast cell degranulation is critical for developing medicines for allergic diseases.

Mast cell-mediated anaphylaxis involves aggregation by FcεRI receptors [9,10]. Lyn triggers FcεRI receptor tyrosine phosphorylation and further mediates Syk and LAT phosphorylation. In addition, LAT and phosphatidylinositol 3-kinase (PI3K) mediate PLCG-2 recruitment and tyrosine phosphorylation [11], leading to activation of calcium signals *in vivo* [12]. NF-κB65, AKT-Nrf2 and p38MAPK have been shown to be involved in mast cell activation [13]. As an important transcription factor, NF-κB regulates the early immune response and various stages of the inflammatory response. AKT pathway is important for cell survival and apoptosis [14]. Allergic inflammation caused by the PI3K/Akt, MAPK, NF-κB and Nrf2/HO-1 pathways plays a key role in activating degranulation and inflammatory factor release of mast cells [15].

Ginsenoside, a steroid compound, is the active ingredient of Ginseng [16]. It affects multiple metabolic pathways, and thus its functions are quite complicated [17]. However, ginsenosides are difficult to isolate and their monomer composition is very unstable. Ginsenoside Rh2 (G-Rh2), which is extracted from ginsenosides, has good chemical stability [18]. Now, we know that ginsenoside Rh2 has anti-inflammatory and anticancer effects. For example, G-Rh2 relieves sensitive airway inflammation in asthmatic mice through NF-κB and MAPK signaling pathways [19]. In addition, G-Rh2 inhibits NF-κB pathway to improve allergic dermatitis [20]. G-Rh2 acts as an anticancer drug by strongly inhibiting cell viability and metastatic processes [21,22]. Moreover, G-Rh2 cooperates with SMI-4a to exert anti-melanoma activity through the AKT/mTOR pathway [23], and that G-Rh2 blocks cancer gene promoter activation by inhibiting the activity of NF-κB and significantly downregulated the expression of IAPs [24]. However, the role of G-Rh2 on mast cell-mediated anaphylaxis remains unclear.

Here, in this study, we investigated the effect of G-Rh2 on mast cell-mediated anaphylaxis. The underlying mechanisms were also analyzed and discussed. Our findings may provide basis for the treatment of anaphylaxis in the future.

2. Materials and methods

2.1. Animals

BALB/c mice (male, n = 50) aged 7 weeks and Sprague-Dawley rats (male, 220 ± 20 g, n = 20) (Medical Department of Yanbian University, Yanji, China) were kept in SPF environment. All animal experiment procedures were approved by the Animal Protection Committee of Yanbian University.

2.2. Asthma model

Mice were allocated into Control group (Control, n = 10), ovalbumin (OVA) group (n = 10), OVA + G-Rh2 25 mg/kg group (OVA + G-Rh2 25) (n = 10), OVA + G-Rh2 50 mg/kg group (OVA + G-Rh2 50) (n = 10), and OVA + G-Rh2 100 mg/kg group (OVA + G-Rh2 100) (n = 10), randomly. Mice in OVA group and OVA + G-Rh2 25/50/100 groups were sensitized by intrapulmonary injection of sensitizing solution (200 μL) on the 1st, 7th and 14th day. The sensitizing solution included 10 μg OVA (Sigma-Aldrich, USA), 1 μg aluminium hydroxide (Imject® Alum, Pierce, USA), and physiological saline. In the control group, 200 μL saline was injected intraperitoneally on the 1st, 7th and 14th day. The bronchial provocation test was performed in OVA mice from the 21st to the 23rd day. Briefly, the mice inhaled 1 % OVA aerosol (the diameter of aerosol particles was about 3–5 μm by ultrasonic nebulizer) once a day for 20 min each time. The control group was exposed to aerosolized saline inhalation. On the 17th day, the OVA + G-Rh2 25/50/100 groups were given G-Rh2 (Sigma, ref. 73,658; 25, 50, 100 mg/kg body weight) orally once a day for 7 consecutive days. At 24 h after the last challenge, the mice were sacrificed.

2.3. Sample collection

After anesthesia, blood samples were immediately collected. Then, the mice were intubated and the lungs were rinsed with 1 mL of pre-chilled PBS to collect bronchoalveolar lavage fluid (BALF). Finally, lung tissue was collected after sacrifice.

2.4. Lung histology and morphology analysis

The lung tissues of mice were processed into 3 μm sections. Toluidine blue staining was used to observe the mast cell. H&E staining was used to observe the infiltration of inflammatory cells around the airway, and PAS staining was used to observe the mucus secretion of goblet cells. Three sections were randomly selected from each mouse, and bronchioles were selected for microscopic observation.

2.5. ELISA

Levels of TNF-α, IL-4, IL-8 and IL-1β in BALF and in RBL-2H3 cells were detected with corresponding ELISA kits (R&D systems, USA). The IgE in mouse serum were also analyzed with an ELISA Kit (Cat # EMIGHE, Invitrogen). The activity of PI3K was quantified by a PI3-Kinase Activity ELISA kit (Echelon, K-1000s). The absorbance was detected at 450 nm wavelength.

2.6. Passive cutaneous anaphylaxis test and ear section staining

The Control group (Control), IgE + Ag group (IgE + Ag), IgE + Ag + G-Rh2 25 mg/kg group (IgE + Ag + G-Rh2 25), IgE + Ag + G-Rh2 50 mg/kg group (IgE + Ag + G-Rh2 50), and, IgE + Ag + G-Rh2 100 mg/kg group (IgE + Ag + G-Rh2 100) were set up, with 10 mice in each group. IgE + Ag + G-Rh2 groups received G-Rh2 once daily for 4 weeks. After 24 h of the last administration, mice in IgE + Ag and IgE + Ag + G-Rh2 groups were sensitized with 0.2 μg anti-DNP IgE in 20 μL PBS. One day later, mice in G-Rh2 groups were injected with 1 mg DNP-HSA intravenously and 1 % evansblue (1:1) mixture subcutaneously. Control group received the same amount of normal saline. At 30 min after the challenge, the mice were anesthetized. A digital micrometer (Mitutoyo 7326, Tokyo, Japan) was used to detect ear thickness.

After determining the thickness, the ears of mice were fixed, sectioned and stained with H&E. The staining was carried out in accordance with the routine procedure. Under the condition of 100 × , 5 regions were randomly selected to count mast cells.

2.7. Cells preparation, culture and treatment

After anesthesia with ether, rats received intraperitoneal injection of 10 mL Ca^{2+} Tyrode buffer. Then, the abdomen was opened under sterile conditions. Peritoneal lavage fluid was collected and rat peritoneal mast cells (RPMCs) purified using Percoll density gradient centrifugation (Pharmacia, Uppsala, Sweden). Toluidine blue staining assessed RPMCs purity.

RBL-2H3 cells (ATCC, USA) and RPMCs were cultured with 5 % CO_2 at 37 °C in 85 % DMEM and 10 % fetal bovine serum. Control

group, IgE + Ag group and G-Rh2 groups were set up. The control group was untreated. IgE + Ag group was incubated with 10 μg/mL anti-DNP IgE for 6 h and then with DNP-HSA (100 ng/mL) for 10 min. In G-Rh2 groups, G-Rh2 (5, 10, 20 μM) was added and incubated at 37°Cfor 30 min. Then, cells were challenged with anti-DNP IgE and DNP-HSA as those in IgE + Ag group.

2.8. Cell viability

After treatment with different concentrations (0, 1, 10, 50, and 100 μM) of G-Rh2, RPMCs and RBL-2H3 cells were cultured in 96-well plate (2×10^4/well). After MTT treatment, absorbance was measured at 570 nm by SpectraMax Gemini®EM (Molecular devices, CA, USA).

2.9. ^{45}Ca uptake measurement

Calcium absorption in Ca^{2+} buffer solution was determined by the method described previously [25]. After incubation at 4 °C for 10 min, the cells of control group, IgE + Ag group and G-Rh2 groups were treated as above described. Finally, the cells were lysed with 10 % Triton X-100. The Liquid Scintillation Analyzer (Canberra Industries, Inc., Meriden, CT, USA) measured the radioactivity.

2.10. Histamine and degranulation measurement

RBL-2H3 cells (5×10^5/well) were treated with anti-DNP IgE (50 ng/mL) overnight. Cells were pretreated with or without G-Rh2 (0.1, 1, 10, 100 μM) for 1 h, and then treated with DNP-HSA (100 ng/mL) for 4 h. After centrifugation for 5 min at 150 g × , 4 °C, the supernatant was collected to determine histamine level by radioenzyme method.

The hypertrophic release of β-hexosaminase is also widely used as a marker of degranulation of mast cells. The release of β-hexosaminase in BALF and by RBL-2H3 cells was measured. Briefly, after incubating BALF with or without G-Rh2 (10, 20, 40 μM) at 37 °C for 30 min, the BALF supernatant was collected. The RBL-2H3 cells were incubated with or without G-Rh2 (0.1, 1, 10, 100 μM) at 37 °C for 1 h. Then, β-hexosaminidase substrate was added. After the reaction was stopped, the degranulation degree of mast cells was detected by spectrophotometer with a wavelength of 405 nm with the addition of β-hexosaminase substrate.

2.11. Immunohistochemistry

Lung tissue sections were immune-stained sequentially with Tryptase (# 19523S; CST), p-Syk (PA5-104904; Thermo Fisher), p-Lyn (PA5-99355; Thermo Fisher) and goat anti-rabbit IgG-HRP (G-21234; Thermo Fisher). RPMCs were immune-stained sequentially with IL-4 (Abcam, USA) and goat anti-mouse IgG-HRP (Abcam). Then, the slides were counterstained and observed under microscope.

2.12. Western blot

Total proteins, cytosol proteins and nuclear proteins were isolated from RBL-2H3 cells. The proteins were subjected to SDS-PAGE and then transferred to membranes. After blocking, the membranes were incubated with Lyn (#2796), p-Lyn (#2731), Fyn (#4023), p-Fyn (#70926), Syk (#2712), p-Syk (#2710), LAT (#9166), p-LAT (#3584), PLCγ2 (#3872), p-PLCγ2 (#3871), PI3K (#17366), p-PI3K (#4228), Raf-1 (#9422), ERK1/2 (#9102), p-ERK1/2 (# 4370), p65 (#8242), AKT (#2920), p-AKT (#9611), p38 (#8690), p-p38 (#4511), Nrf2 (#12721), Keap1 (#4678), GAPDH (#2118), and PCNA (#13110) at room temperature for 1 h. These antibodies were from CST (Danvers, MA, USA). The HRP conjugated secondary antibody was then added for incubation. GAPDH and PCNA were used as internal references. Relative level of protein was calculated relative to GAPDH or PCNA.

2.13. PP2 treatment

After treating with 25 ng/mL DNP-HAS, RBL-2H3 cells were incubated with or without G-Rh2 (5, 10, 20 μM) or PP2 (20 μM) for 10 min.

2.14. siRNA transfection

After transfection with 100 nM siAKT (#6909; CST), siNrf2 (#5285; CST), sip 65 (#6337; CST) or siControl (#6568; CST) for 48 h, RBL-2H3 cells were collected for further analysis.

2.15. Inhibitor treatment

RBL-2H3 cells were treated with MK2206 (AKT inhibitor) or SB 203580 (p38MAPK inhibitor) for 2 h and G-Rh2 for 1 h. Then, cells were collected for further analysis.

2.16. Statistical analysis

Data were analyzed using SPSS 17.0. Data of 5 independent experiments were shown as means ± standard error (SEM). One-way analysis of variance and Duncan's multiple range tests were performed. $P < 0.05$ indicates statistically significant difference.

3. Results

3.1. Effect of G-Rh2 on OVA-mediated asthma in mice

Mast cells are mainly distributed in human skin, airways, and digestive tract. In this study, we detected tryptase expression in lung tissues to represent mast cells. It was found that the mast cells in the lung tissue of the asthma group could be stained, indicating that there was an inflammatory reaction in the mast cells of the asthma group, while the G-Rh2 reduced inflammation. The expression of tryptase in the OVA group increased, while G-Rh2 inhibited the expression of tryptase (Fig. 1A). H&E staining was used to assess the infiltration of inflammatory cells in lung tissue. The results showed that compared with the Control group, inflammatory cells infiltrated extensively around the trachea and blood vessels in the OVA group. However, G-Rh2 treatment relieved this situation (Fig. 1B). The goblet cell proliferation and mucus secretion were evaluated by PAS staining. Compared with mice in the Control group, mice in the OVA group had obvious proliferation of goblet cells around the airway and increased mucus secretion (Fig. 1C). G-Rh2 treatment obviously inhibited airway goblet cell proliferation and mucus secretion in asthmatic mice. The immunohistochemical method was used to observe the expression of p-Lyn, and p-Syk. As shown in Fig. 1D, the expression levels of p-Lyn and p-Syk in the OVA group were higher than those in the control group. We found that G-Rh2 inhibited the expression levels of p-Lyn and p-Syk in a dose-dependent manner. In addition, the levels of TNF-α, IL-4, IL-8 and IL-1β in OVA group were significantly higher compared to Control group (Fig. 1E). Compared with the OVA group, G-Rh2 reduced the production of TNF-α, IL-4, IL-8 and IL-1β in asthmatic mice dose dependently. In Fig. 1F, compared with OVA

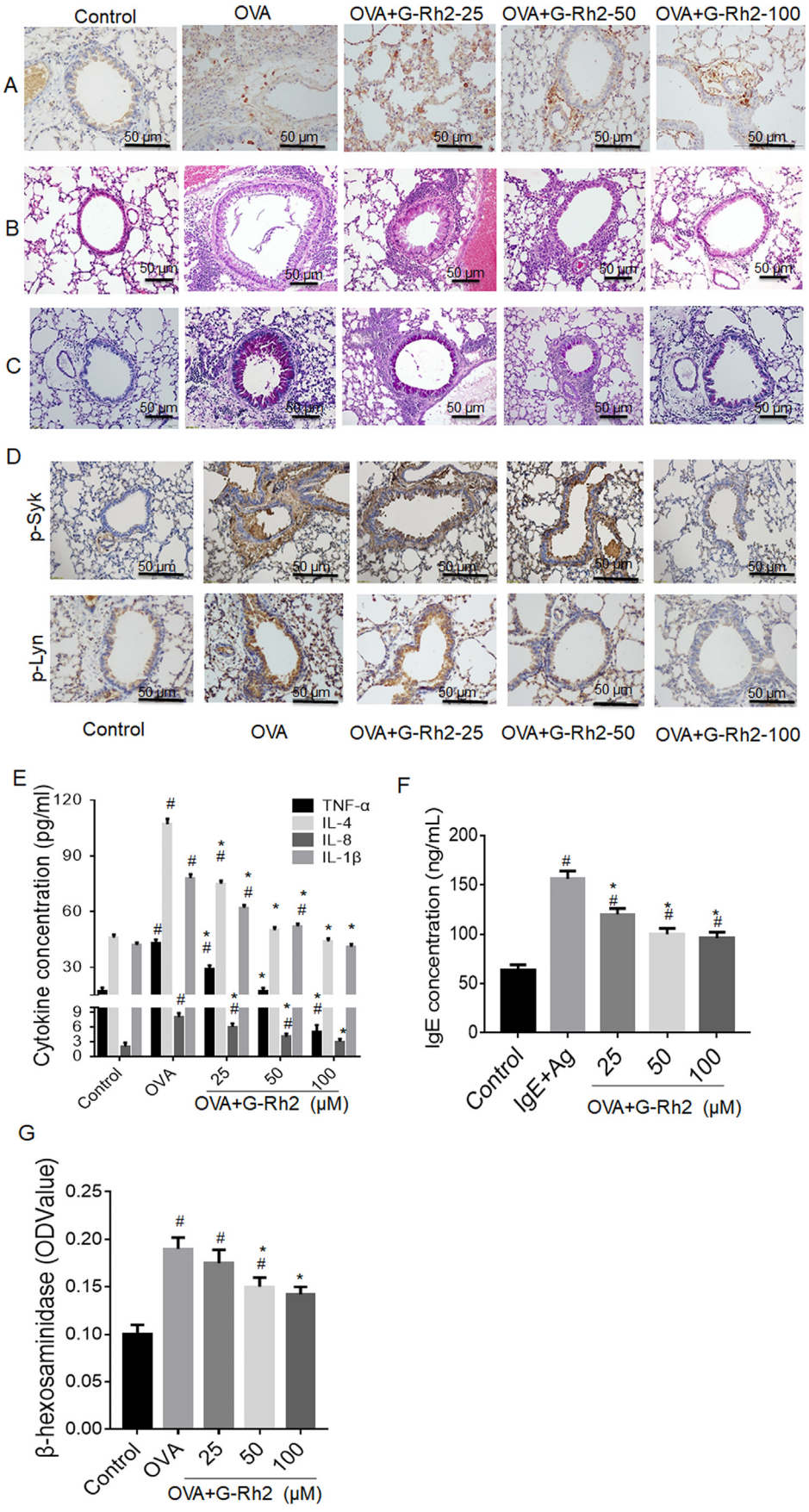

Fig. 1. Effects of G-Rh2 on OVA-mediated asthmatic mice. (A) Immunohistochemical staining of tryptase in lung tissue. (B) H&E staining of mouse lung sections. (C) PAS staining of mouse lung sections. (D) Immunohistochemical staining of p-Lyn and p-Syk proteins in lung tissue. (E) Changes of cytokines in alveolar lavage fluid of asthmatic mice. (F) Changes in serum IgE in the OVA-asthma mice model. (G) The content of β-hexosaminase in BALF. Each data value represents the average of 5 independent experiments (±S.E.M.).*$P < 0.05$ vs. the Control group. #$P < 0.05$ vs. the OVA group.

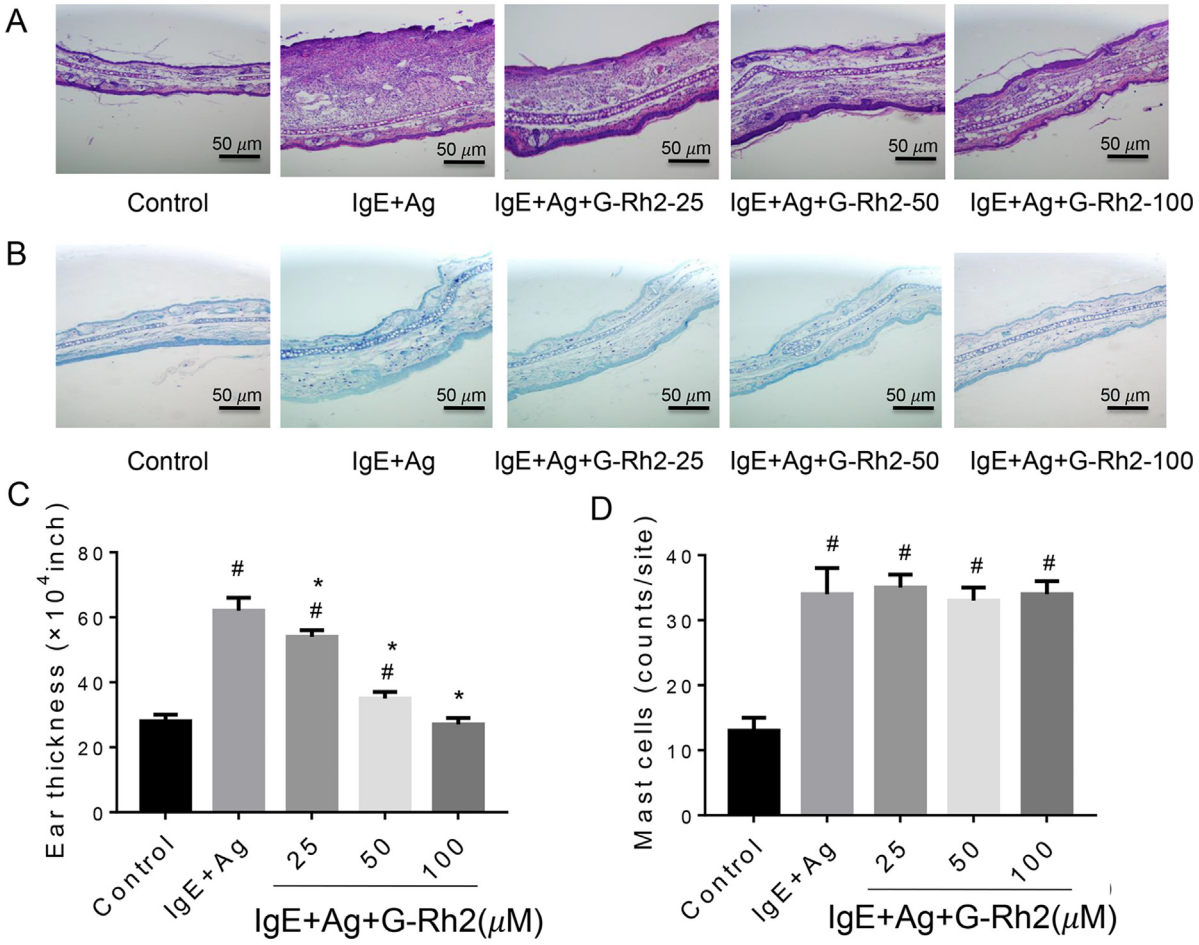

Fig. 2. The effect of G-Rh2 on ear swelling in mice. Mice were divided into Control group, IgE + Ag group and IgE + Ag + G-Rh2 groups. Representational photographs of ear sections stained with H&E (A) and toluidine blue (B) were shown. (C) Ear thickness was measured by dial thickness meter. (D) Mast cells were counted in the dermis. Each data value represents the average of 5 independent experiments (±S.E.M.). #$P < 0.05$ vs. the Control group. *$P < 0.05$ vs. the IgE + Ag group.

group, G-Rh2 dose dependently reduced the production of IgE in serum of asthmatic mice. Moreover, G-Rh2 also inhibited the expression of β-hexosaminase in BALF dose dependently (Fig. 1G). Therefore, we speculate that G-Rh2 inhibits the OVA mediated allergic reaction of asthma in mice and that this effect may be achieved by inhibiting Lyn and Syk activation and mast cell degranulation.

3.2. The effect of G-Rh2 on ear swelling in mice

To study the effect of G-Rh2 on allergic ear swelling, H & E and toluidine blue staining were used. H & E staining results showed that the auricles of the mice in the IgE + Ag group became thicker, edema, and had a large number of inflammatory cell infiltration (Fig. 2A). However, the G-Rh2 group significantly alleviated the aforementioned pathological changes dose dependently. In addition, G-Rh2 also reduced ear swelling caused by allergic reactions and significantly reduced ear thickness dose dependently (Fig. 2B and C). Mast cell infiltration in the ears of mice in the IgE + Ag group was significantly increased than Control group (Fig. 2D). Moreover, G-Rh2 treatment did affect the number of mast cells. Therefore, G-Rh2 reduces inflammation and swelling induced by the allergic responses, but not via regulating the number of mast cells.

3.3. Effects of G-Rh2 on uptake of calcium, degranulation, histamine release, and pro-inflammatory cytokine expression in IgE-sensitized mast cells

First, we used MTT to explore the effect of G-Rh2 on cell viability. The results showed that cell survival was not significantly different at different concentrations of G-Rh2, suggesting that G-Rh2 had no cytotoxicity at the experimental concentrations (Fig. 3A). Meanwhile, we studied the effect of G-Rh2 on mast cell morphology. The surface of normal RPMCs was regular, round and filled with granules (Fig. 3B). After treatment with IgE + Ag, the surface of RPMCs became irregular. RPMCs swelled and the number of granules increased. However, after treatment with G-Rh2, RPMC became slightly larger than normal cells. The cell surface became round and the granularity decreased.

Next, we investigated the effect of G-Rh2 on calcium uptake. The result showed that calcium uptake in RPMCs and RBL-2H3 cells was significantly higher after IgE + Ag treatment (Fig. 3C and D). However, G-Rh2 significantly inhibited this increase dose dependently ($P < 0.05$ or $P < 0.01$). We therefore concluded that G-Rh2 inhibited IgE-mediated uptake of calcium.

The inhibitory effect of G-Rh2 on histamine release and degranulation of IgE sensitized mast cells was also analyzed. The results showed that histamine release and degranulation in RBL-2H3 cells in the IgE group were significantly increased compared to the control group (Fig. 3E and F). However, in IgE-sensitized RBL-

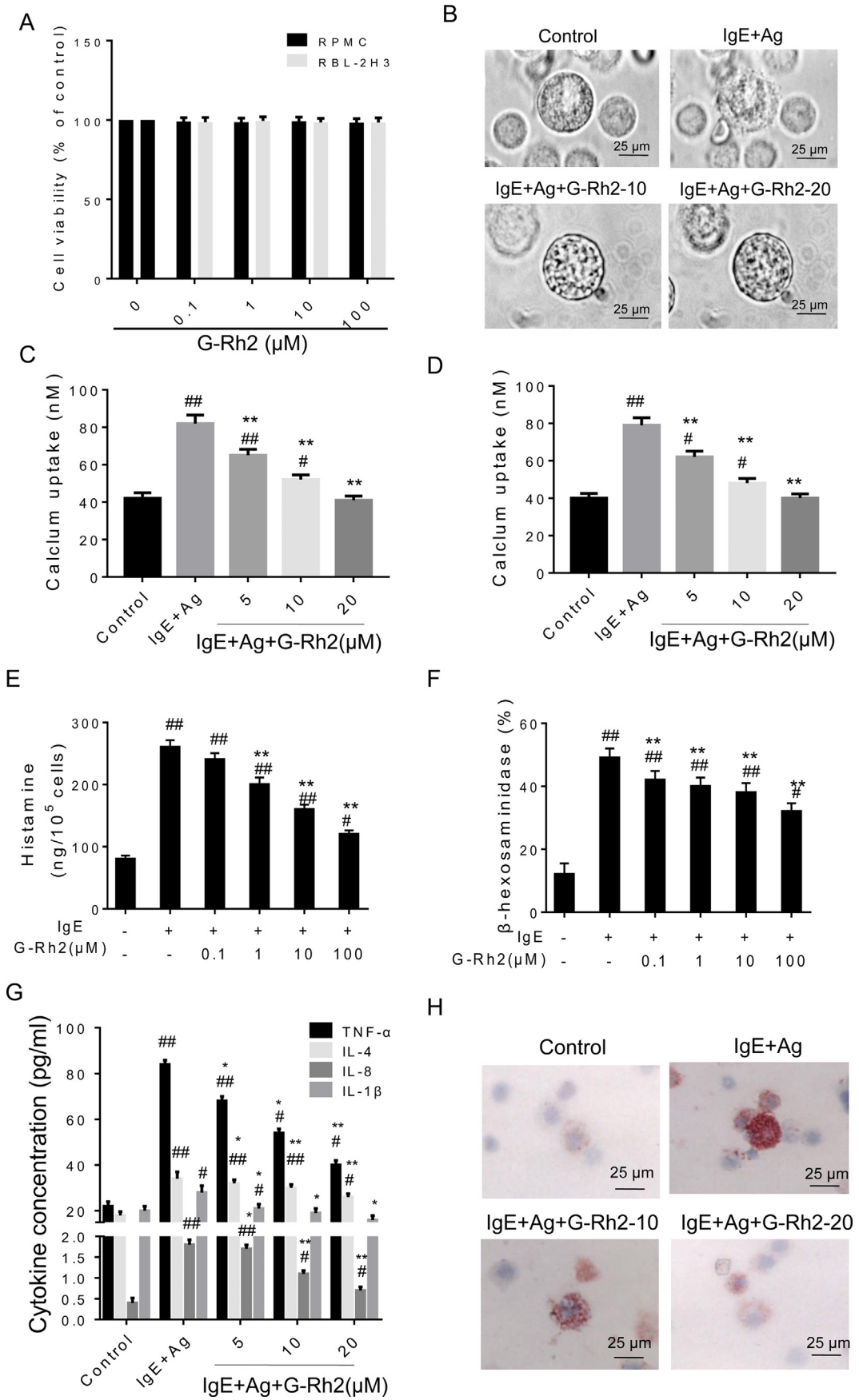
A
Cell viability (% of control)
RPMC
RBL-2H3
G-Rh2 (μM)
B
Control
IgE+Ag
IgE+Ag+G-Rh2-10
IgE+Ag+G-Rh2-20
25 μm
C
Calcium uptake (nM)
Control
IgE+Ag
IgE+Ag+G-Rh2(μM)
D
Calcium uptake (nM)
E
Histamine (ng/10^5 cells)
IgE
G-Rh2(μM)
F
β-hexosaminidase (%)
G
Cytokine concentration (pg/ml)
TNF-α
IL-4
IL-8
IL-1β
H

2H3 cells, G-Rh2 inhibited the release and degranulation of histamine dose dependently.

In addition, we examined the effect of G-Rh2 on cytokine release by ELISA. As shown in Fig. 3G, cytokine levels in the IgE + Ag group were significantly higher. However, G-Rh2 had a significant inhibitory effect on cytokine release dose dependently. IgE-treated RPMCs had obviously higher IL-4 while G-Rh2 treatment reduced IL-4 level (Fig. 3H). These results indicate that G-Rh2 inhibits histamine release, degranulation and proinflammatory cytokine expression in IgE-sensitized mast cells dose dependently.

3.4. Effects of G-Rh2 on FcεRI signaling pathway in IgE-sensitized RBL-2H3 cells

The activity of kinases, including Fyn and Lyn, is the key to activating Syk in antigen-stimulated mast cells. Thus, the levels of Fyn and Lyn were measured by Western blot *in vitro* to determine which tyrosine kinase is the direct target of G-Rh2 in mast cells. Compared to control, the level of p-Fyn and p-Lyn in the IgE + Ag group increased significantly. G-Rh2 acted on p-Lyn in a concentration-dependent manner *in vitro* but had no effect on p-Fyn (Fig. 4A), suggesting that Lyn is the target of G-Rh2 in mast cells.

In order to study the mechanism of G-Rh2 underlying its inhibitory effect on mast cell activation, we investigated its effect on the levels of early signaling proteins (including Syk and LAT) in IgE-sensitized RBL-2H3 cells. Compared to the control group, we found increased levels of Syk and LAT phosphorylation in the IgE group (Fig. 4B). However, G-Rh2 inhibited phosphorylation of Syk and LAT in a dose-dependent manner. PP2, which is a well-known inhibitor of Src family kinases and inhibits the phosphorylation of Syk and LAT, served as a positive control. Then, the effect of G-Rh2 on protein expression (including PLCr2 and PI3K) after mast cell activation was analyzed. The levels of phosphorylation of PLCr2 and PI3K in IgE-sensitized RBL-2H3 cells were increased than control group (Fig. 4C). We found that G-Rh2 inhibited the phosphorylation levels of PLCr2 and PI3K dose dependently. The activity of PI3K was quantified by a PI3-Kinase Activity ELISA kit. As shown in Fig. 4D, the activity of PI3K in RBL-2H3 cells sensitized with IgE was higher than that in the Control group. G-Rh2 inhibited PI3K activity in a dose-dependent manner. In Fig. 4E, the expression levels of Raf-1 and p-ERK1/2 in IgE-sensitized RBL-2H3 cells were higher than those in the Control group. We found that G-Rh2 inhibited the expression levels of Raf-1 and p-ERK1/2 in a dose-dependent manner. Thus, G-Rh2 dose dependently inhibits the FcεRI signaling pathway in IgE-sensitized RBL-2H3 cells.

3.5. Effects of G-Rh2 on AKT-Nrf2/NF-κBp65 and p38-Nrf2/NF-κBp65 signal pathways in IgE-sensitized RBL-2H3 cells

We examined the effect of G-Rh2 on p-AKT, p-p38 and Nrf2 in IgE-sensitized RBL-2H3 cells by Western blotting. Compared to control, the levels of p-AKT and p-p38 were up-regulated, while the level of Keap1 was down-regulated in IgE-sensitized RBL-2H3 cells (Fig. 5A). After treating mast cells with G-Rh2 (5, 10, 20 μM), p-AKT and p-p38MAPK levels were down-regulated, while the level of Keap1 was up-regulated. In addition, the level of Nrf2 in the nucleus of the IgE + Ag group increased significantly, and that in the G-Rh2 groups increased significantly than that in control and IgE + Ag groups. However, the expression of Nrf2 in the cytoplasm is opposite to that in the nucleus. Together, G-Rh2 reduced the expression of p-AKT, p-p38 and Nrf2 (cytoplasm) and increased the level of Keap1 in IgE-sensitized RBL-2H3 cells.

Western blot was performed to detect cytosol and nuclear NF-κBp65 level. After sensitization of RBL-2H3 cells by IgE, the level of NF-κBp65 in the nucleus was significantly increased, while the level of NF-κBp65 in the cytoplasm was significantly reduced (Fig. 5A). However, after treatment with G-Rh2, the level of NF-κBp65 in the nucleus decreased significantly, while the level of cytoplasmic NF-κBp65 recovered. In a word, G-Rh2 inhibited the activation of NF-κBp65 by inhibiting the nuclear translocation of the p65 subunit.

G-Rh2 may have certain effects on the AKT-Nrf2 signaling pathway of IgE-sensitized RBL-2H3 cells. We found that knockdown of AKT inhibited phosphorylation of NF-κB-p65, and knockdown of Nrf2 inhibited phosphorylation of NF-κB-p65 (Fig. 5B). However, we found that knockdown of NF-κB-p65 had no significant effect on AKT (Fig. 5B), confirming the upstream and downstream relationship between Akt and NF-κB-p65. To investigate whether AKT affects the effect of G-Rh2 on Nrf2, we further pretreated RBL-2H3 cells with MK2206 (AKT inhibitor) or BT (Nrf2 inhibitor). The results showed that MK2206 inhibited the expression of p-AKT and Nrf2, while BT inhibited the expression of Nrf2. We found p-AKT and Nrf2 were activated after the G-Rh2 treatment of RBL-2H3 cells. G-Rh2+MK2206 effectively inhibited p-AKT and Nrf2 activation. We also found that G-Rh2+BT suppressed Nrf2 activation (Fig. 5C). These results indicate that G-Rh2 regulates AKT-Nrf2 signaling in IgE-sensitized RBL-2H3 cells.

Meanwhile, G-Rh2 may also have effects on p38-Nrf2 signal axis of RBL-2H3 cells sensitized by IgE. We observed that knockdown of p38MAPK inhibited NF-κB-p65 phosphorylation (Fig. 5D). Knockdown of Nrf2 reduced the phosphorylation of NF-κB-p65, but the knockdown of NF-κB-p65 has no significant effect on AKT (Fig. 5D). To investigate whether G-Rh2 was regulated by p38, RBL-2H3 cells were pretreated with SB 203580 (p38MAPK inhibitor) or BT (Nrf2 inhibitor). Subsequently, SB 2035806 inhibited the expression of p-p38 and Nrf2, while BT inhibited the expression of Nrf2. After treating RBL-2H3 cells with G-Rh2, we found that p-p38 and Nrf2 were activated. We observed that treatment with G-Rh2+SB 203580 effectively blocked the activation of Nrf2 and p-p38 in RBL-2H3 cells, and that G-Rh2+BT also effectively blocked the expression of Nrf2 (Fig. 5E). In conclusion, G-Rh2 activated the p38-Nrf2 signal pathway of RBL-2H3 cells sensitized by IgE.

4. Discussion

Previous studies have reported that G-Rh2 has antioxidant, anti-inflammatory, and anti-apoptotic activities [26–29]. Here we demonstrate the anti-allergic effects of G-Rh2 by activating AKT-Nrf2 and p38MAPK-Nrf2 *in vivo* and *in vitro*. Asthma is a common allergic disease currently, and severely affects the normal life of patients at the time of onset [30]. Mast cells are involved in the development of asthma, and cytokines such as IL-1β, TNF-α, IL-8,

Fig. 3. Effects of G-Rh2 on uptake of calcium, histamine release, degranulation and pro-inflammatory cytokine expression in IgE-sensitized mast cells. (A) Purified RPMCs and RBL-2H3 cells were treated with different concentrations of G-Rh2. Cell viability was measured by MTT assay. (B) Morphology of IgE-mediated degranulation of RPMCs (1000× magnification). Control group: Normal RPMCs in HEPES-Tyrode buffer; IgE + Ag group: RPMCs sensitized with 10 g/mL anti-DNP IgE for 6 h and challenged with 100 ng/mL DNP-HAS; IgE + Ag + G-Rh2 group: Prior to the challenge with 100 ng/mL DNP-HAS, cells were preincubated with 20 μM G-Rh2 at 37◦C for 30 min. (C) Calcium uptake by radioenzyme method (RPMCs). (D) Calcium uptake by radioenzyme method (RBL-2H3 cells). (E) Histamine levels were measured with a fluorescent plate reader (RBL-2H3 cells). (F) Level of β-hexosaminase Each data value represents the average of 5 independent experiments (±S.E.M.). (G) The expression of cytokines by RBL-2H3 cells was detected by ELISA. (H) Immunohistochemical detection of IL-4 expression in IgE-mediated RPMCs. Each data value represents the average of 5 independent experiments (±S.E.M.). #$P < 0.05$, ##$P < 0.01$ vs. the Control group. *$P < 0.05$, **$P < 0.01$ vs. the IgE + Ag group.

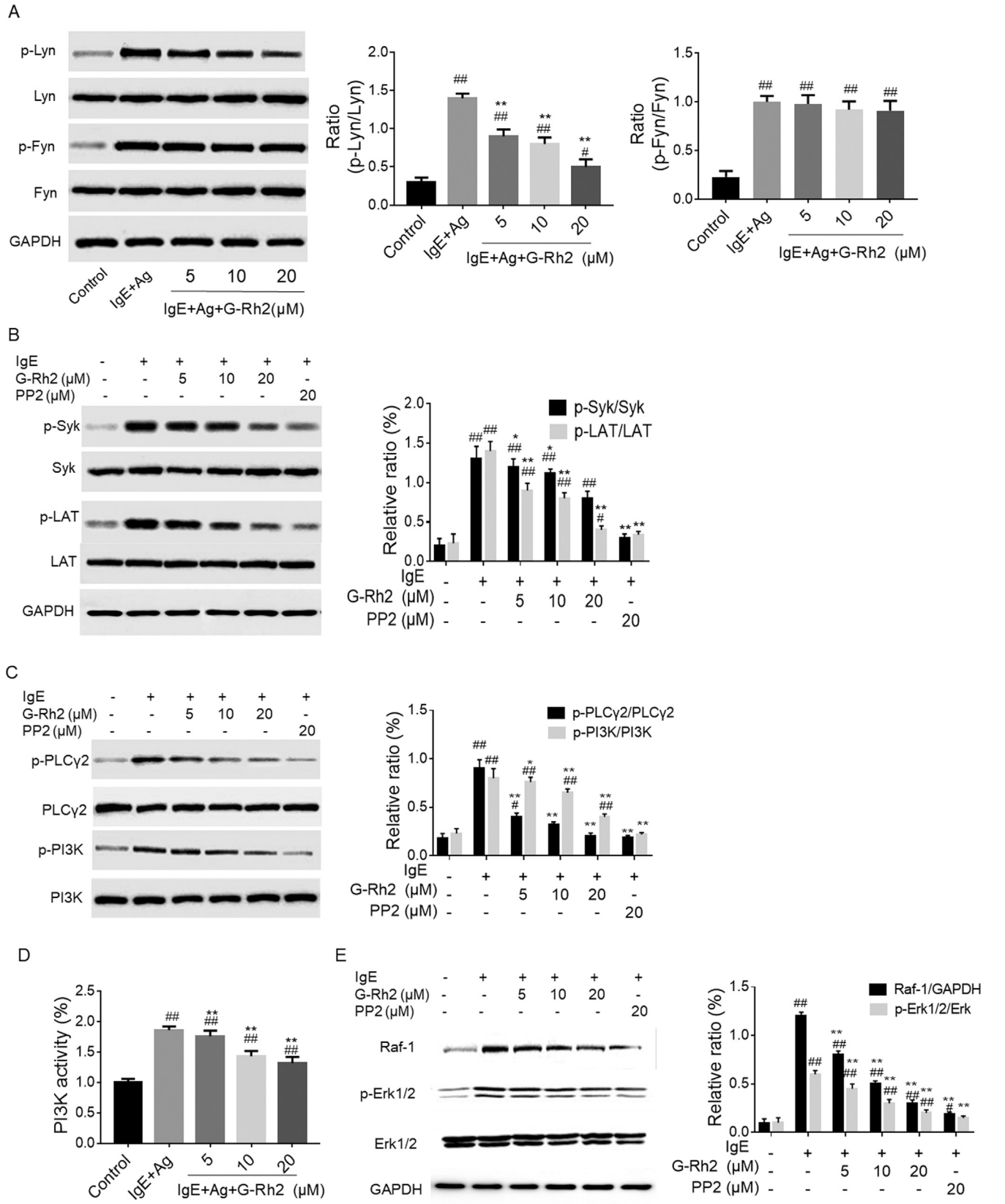

Fig. 4. Effects of G-Rh2 on FcεRI signaling pathway in IgE-sensitized RBL-2H3 cells. (A Western blot was used to detect the expression of p-Lyn, Lyn, p-Fyn, and Fyn protein. RBL-2H3 cells were stimulated with 25 ng/mL DNP-HSA, and then incubated with G-Rh2 or PP2 for 10 min. Protein levels were detected with Western blot. (B) The levels of p-Syk, Syk, p-LAT, and LAT protein. (C) The levels of p-PLCγ2, PLCγ2, p-PI3K, and PI3K protein. (D) The activity of PI3K was quantified by a PI3-Kinase Activity ELISA kit. (E) The levels of Raf-1, p-ERK1/2, and ERK1/2 protein. Each data value represents the average value of 5 independent experiments (±SEM). #$P < 0.05$, ##$P < 0.01$ vs. the Control group. *$P < 0.05$, **$P < 0.01$ vs. the IgE + Ag group.

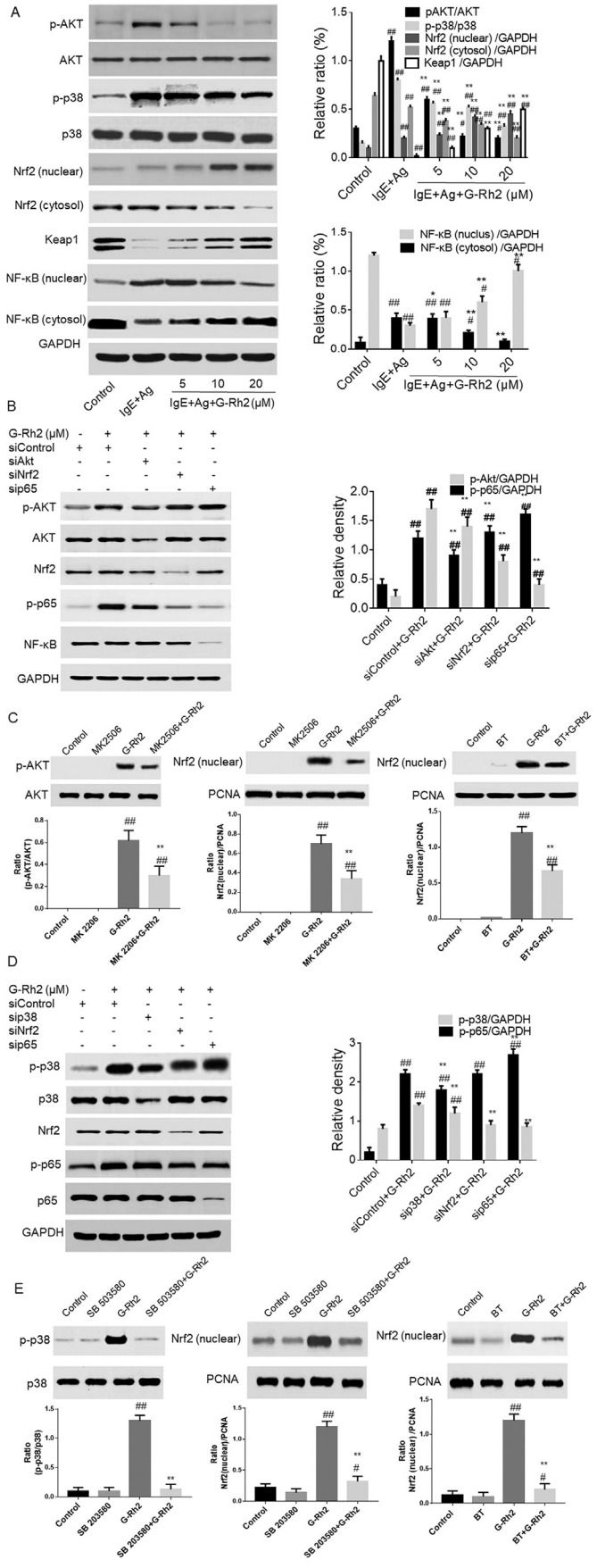

and IL-4 are involved in the development of chronic allergic inflammation [31]. TNF-α promotes T cells to produce various inflammatory factors, which in turn promotes inflammation [32]. IL-4 has immunomodulatory effects on mast cells and can stimulate the proliferation of mast cells [33]. IL-8 can exert chemotactic effects on various cells to the lesion site in the inflammatory response [34]. IL-1β is an inflammatory cytokine, which is widely involved in many pathological processes, such as tissue destruction and edema formation [35]. In this study, we found that the expression of tryptase in the OVA group increased, while this was inhibited by G-Rh2. The activation of Lyn and Syk in the lung tissue of the G-Rh2 administration group also decreased. Moreover, G-Rh2 reduced TNF-α, IL-4, IL-8, and IL-1β produced by mast cells in asthma and inflammatory responses and decreased the production of IgE in serum of OVA induced asthmatic mice, thereby inhibiting the further development of chronic allergic inflammation.

Mast cells are important for allergic inflammation [36,37]. Activated mast cells release histamine, chemokines, and cytokines [38]. In addition, calcium in mast cells is significantly increased after mast cell activation [39]. In this study, we found that G-Rh2 significantly reduced calcium uptake, thereby inhibiting mast cell activation. However, G-Rh2 did not significantly affect the viability or the number of mast cells. In addition, histamine is one of the most important factors for allergic reactions [40]. Our results showed that G-Rh2 also dose dependently inhibited histamine release and degranulation of mast cells. Therefore, we speculate that G-Rh2 inhibits the release and degranulation of histamine by inhibiting the calcium uptake of mast cells dose dependently.

Activation of the FcεRI signaling pathway can cause a variety of allergic reactions [41,42]. The binding of IgE antigen to FcεRI leads to activation of FcεRI [43], which causes various allergic reactions, such as degranulation, cytokine expression and secretion [44]. Antigen-mediated aggregation of FcεRI on mast cells will activate Syk and cause phosphorylation of other mediators (such as LAT, PLCr2, PI3K, etc.) [45,46], and finally, cause mast cells to degranulate and release cytokines [47]. To understand how G-Rh2 inhibits mast cell activation, we investigated the effect of G-Rh2 on FcyRI-mediated Syk and LAT phosphorylation. We found that G-Rh2 inhibited antigen-induced phosphorylation of Lyn, Syk, LAT, PLCr2, PI3K, ERK1/2 and the expression of Raf-1 dose dependently. Moreover, G-Rh2 could inhibit the activity of PI3K induced by IgE in a dose-dependent manner. These findings indicate that G-Rh2 dose dependently significantly inhibits the activation of FcεRI-mediated signaling pathways and thus exerts anti-allergic effects.

In addition, NF-κB-p65 is also involved in mast cell activation [48]. Thus, we further clarified the effect of G-Rh2 on NF-κB-p65. AKT-Nrf2 and p38MAPK-Nrf2 signaling pathways, which have important roles in mast cell activation [49–51]. We found that G-Rh2 inhibited antigen-induced NF-κB-p65, Akt, p38MAPK phosphorylation but up-regulated Keap1 expression in mast cells dose dependently. In addition, knockdown of AKT or p38MAPK significantly reduced phosphorylation of NF-κB-p65, but knockdown of NF-κB-p65 had no significant effect on AKT or p38MAPK, indicating that AKT and p38MAPK affect activation of NF-κB-p65. In summary,

Fig. 5. Effects of G-Rh2 on AKT-Nrf2/NF-κBp65 and p38-Nrf2/NF-κBp65 signal pathways in IgE-sensitized RBL-2H3 cells. Protein levels were detected with Western blot. (A) Levels of p-AKT, AKT, p-p38, p38, Nrf2 and NF-κB. ##$P < 0.01$ vs. the Control group. *$P < 0.05$, **$P < 0.01$ vs. the IgE + Ag group. (B) Levels of p-AKT, AKT, Nrf2, Keap-1, p-p65, and NF-κB. ##$P < 0.01$ vs. the Control group. **$P < 0.01$ vs. the siControl + G-Rh2 group. (C) Levels of p-AKT, AKT, and Nrf2 (nuclear). ##$P < 0.01$ vs. the Control group. **$P < 0.01$ vs. the G-Rh2 group. (D) Levels of p-p38, p38, Nrf2, p-p65, and p65. ##$P < 0.01$ vs. the Control group. **P < 0.01 vs. the siControl + G-Rh2 group. (E) Levels of p-p38, p38, and Nrf2 (nuclear). #$P < 0.05$, ##$p < 0.01$ vs. the Control group. **$P < 0.01$ vs. the G-Rh2 group. Each data value represents the average value of 5 independent experiments (±SEM).

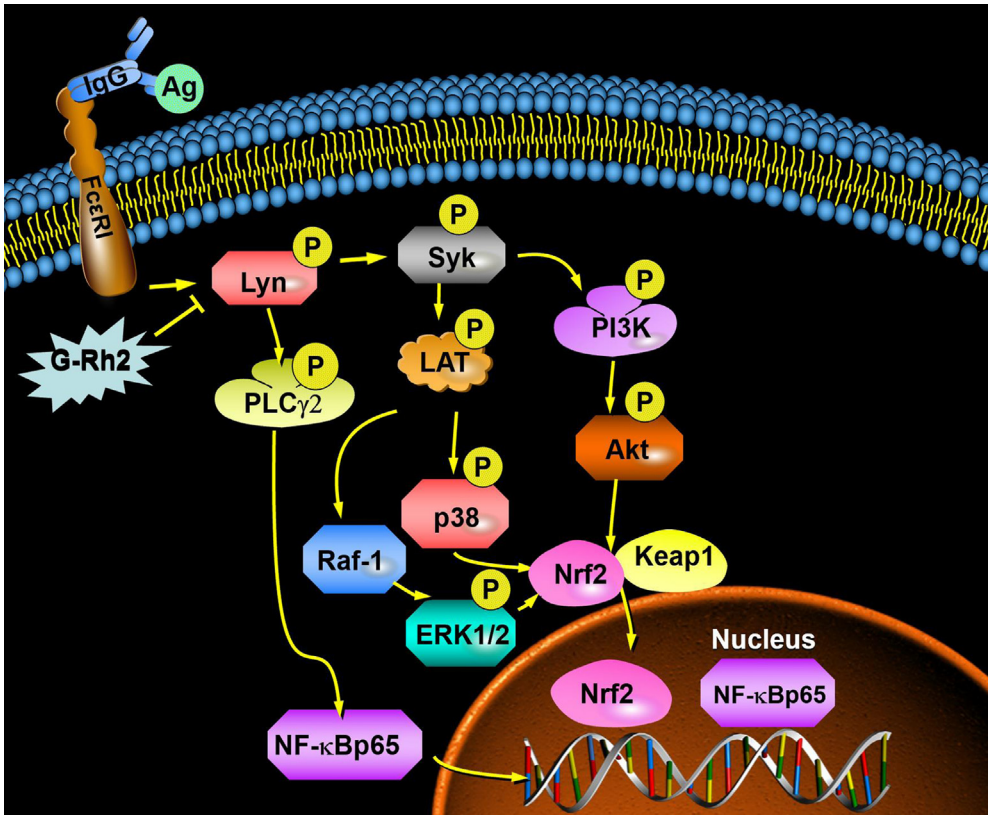

Fig. 6. An illustration of the mechanism underlying the inhibitory effect of G-Rh2 on the FcεRI signal pathway. G-Rh2 blocked IgE-induced mast cell degranulation by inhibiting AKT-Nrf2 and p38MAPK-Nrf2 signal pathways.

we confirmed the relationship between AKT or p38MAPK and Nrf2/NF-κB-p65. G-Rh2 inhibits NF-κB-p65 activation by inhibiting AKT-Nrf2 and p38MAPK-Nrf2 signaling pathways. The possible mechanisms are as follows: 1) Activation of AKT and p38MAPK leads to Nrf2 activation and further to NF-κB-p65 activation; 2) Activation of AKT and p38MAPK results in upregulation of Nrf2 expression and activation of NF-κB-p65; 3) AKT and p38MAPK may regulate the activation of NF-κB-p65 through other signaling molecules.

Based on the results of *in vivo* and *in vitro* experiments, a schematic diagram of the mechanism of G-Rh2 inhibition on the FcεRI signal pathway has been drawn (Fig. 6). G-Rh2 dose dependently blocked IgE-induced mast cell degranulation by inhibiting AKT-Nrf2 and p38MAPK-Nrf2 pathways.

In summary, G-Rh2 reduced calcium uptake and histamine release and inhibited inflammatory cytokines most likely through AKT-Nrf2 and p38MAPK-Nrf2 signal axes. Thus, G-Rh2 might help prevent or treat mast cell-mediated allergic inflammatory diseases.

Funding

This work was supported by National Natural Science Foundation of China (No: 81970018, 81860729, and 82060008), and Jilin Provincial Basic Research Project of Central Guided Local Science and Technology Development Fund (No.: 202002020JC). This work was financially supported by the Higher Education Discipline Innovation Project (111 Project, D18012).

Declaration of competing interest

All authors declare no competing interests.

References

[1] Del Giacco SR, Bakirtas A, Bel E, Custovic A, Diamant Z, Hamelmann E, Heffler E, Kalayci O, Saglani S, Sergejeva S, et al. Allergy in severe asthma. Allergy 2017;72:207–20.
[2] Kuo CH, Collins AM, Boettner DR, Yang Y, Ono SJ. Role of CCL7 in type I hypersensitivity reactions in murine experimental allergic conjunctivitis. J Immunol 2017;198:645–56.
[3] Liu H, Tan J, Liu J, Feng H, Pan D. Altered mast cell activity in response to rhinovirus infection provides novel insight into asthma. J Asthma 2020;57:459–67.
[4] Babina M, Wang Z, Franke K, Guhl S, Artuc M, Zuberbier T. Yin-yang of IL-33 in human skin mast cells: reduced degranulation, but augmented histamine synthesis through p38 activation. J Invest Dermatol 2019;139:1516–25.
[5] Zhou J, Zhang C, Shang J. IL-33 promotes degranulation of mouse bone marrow-derived mast cells and release of cytokines IL-1β, IL-6 and TNF-α, vol. 32; 2016. p. 462–75. Xi Bao Yu Fen Zi Mian Yi Xue Za Zhi.
[6] Buckley MG, Williams CM, Thompson J, Pryor P, Ray K, Butterfield JH, Coleman JW. IL-4 enhances IL-3 and IL-8 gene expression in a human leukemic mast cell line. Immunology 1995;84:410–5.
[7] Furuno T, Shinkai N, Inoh Y, Nakanishi M. Impaired expression of the mitochondrial calcium uniporter suppresses mast cell degranulation. Mol Cell Biochem 2015;410:215–21.
[8] Mazurek N, Berger G, Pecht I. A binding site on mast cells and basophils for the anti-allergic drug cromolyn. Nature 1980;286:722–3.
[9] Méndez-Enríquez E, Hallgren J. Mast cells and their progenitors in allergic asthma. Front Immunol 2019;10:821.
[10] Gast M, Preisinger C, Nimmerjahn F, Huber M. IgG-independent Co-aggregation of FcεRI and FcγRIIB results in LYN- and SHIP1-dependent tyrosine phosphorylation of FcγRIIB in murine bone marrow-derived mast cells. Front Immunol 2018;9:1937.
[11] Suurmond J, Habets KLL, Tatum Z, Schonkeren JJ, Hoen PAC, Huizinga TWJ, Laros JFJ, Toes REM, Kurreeman F. Repeated FcεRI triggering reveals modified mast cell function related to chronic allergic responses in tissue. J Allergy Clin Immunol 2016;138:869–80.
[12] Chen YC, Chang YC, Chang HA, Lin YS, Tsao CW, Shen MR, Chiu WT. Differential Ca(2+) mobilization and mast cell degranulation by FcεRI- and GPCR-mediated signaling. Cell Calcium 2017;67:31–49.
[13] Kempuraj D, Thangavel R, Selvakumar GP, Ahmed ME, Zaheer S, Raikwar SP, Zahoor H, Saeed D, Dubova I, Giler G, et al. Mast cell proteases activate

astrocytes and glia-neurons and release Interleukin-33 by activating p38 and ERK1/2 MAPKs and NF-κB. Mol Neurobiol 2019;56:1681–93.
[14] Miao Y, Jiang M, Qi L, Yang D, Xiao W, Fang F. BCAP regulates dendritic cell maturation through the dual-regulation of NF-κB and PI3K/AKT signaling during infection. Front Immunol 2020;11:250.
[15] Ye J, Piao H, Jiang J, Jin G, Zheng M, Yang J, Jin X, Sun T, Choi YH, Li L, et al. Polydatin inhibits mast cell-mediated allergic inflammation by targeting PI3K/Akt, MAPK, NF-κB and Nrf2/HO-1 pathways. Sci Rep 2017;7:11895.
[16] Cui CH, Jeon BM, Fu Y, Im WT, Kim SC. High-density immobilization of a ginsenoside-transforming β-glucosidase for enhanced food-grade production of minor ginsenosides. Appl Microbiol Biotechnol 2019;103:7003–15.
[17] Gao Y, Wang T, Wang G, Li G, Sun C, Jiang Z, Yang J, Li Y, You Y, Wu X, et al. Preclinical safety of ginsenoside compound K: acute, and 26-week oral toxicity studies in mice and rats. Food Chem Toxicol 2019;131:110578.
[18] Kim YJ, Perumalsamy H, Castro-Aceituno V, Kim D, Markus J, Lee S, Kim S, Liu Y, Yang DC. Photoluminescent and self-assembled hyaluronic acid-zinc oxide-ginsenoside Rh2 nanoparticles and their potential caspase-9 apoptotic mechanism towards cancer cell lines. Int J Nanomed 2019;14:8195–208.
[19] Li LC, Piao HM, Zheng MY, Lin ZH, Choi YH, Yan GH. Ginsenoside Rh2 attenuates allergic airway inflammation by modulating nuclear factor-κB activation in a murine model of asthma. Mol Med Rep 2015;12:6946–54.
[20] Ko E, Park S, Lee JH, Cui CH, Hou J, Kim MH, Kim SC. Ginsenoside Rh2 ameliorates atopic dermatitis in NC/nga mice by suppressing NF-kappaB-Mediated thymic stromal lymphopoietin expression and T helper type 2 differentiation. Int J Mol Sci 2019;20:6111.
[21] Zhu C, Liu F, Qian W, Zhang T, Li F. Combined effect of sodium selenite and ginsenoside Rh2 on HCT116 human colorectal carcinoma cells. Arch Iran Med 2016;19:23–39.
[22] Ma J, Gao G, Lu H, Fang D, Li L, Wei G, Chen A, Yang Y, Zhang H, Huo J. Reversal effect of ginsenoside Rh2 on oxaliplatin-resistant colon cancer cells and its mechanism. Exp Ther Med 2019;18:630–46.
[23] Lv DL, Chen L, Ding W, Zhang W, Wang HL, Wang S, Liu WB. Ginsenoside G-Rh2 synergizes with SMI-4a in anti-melanoma activity through autophagic cell death. Chin Med 2018;13:11.
[24] Wang YS, Lin Y, Li H, Li Y, Song Z, Jin YH. The identification of molecular target of (20S) ginsenoside Rh2 for its anti-cancer activity. Sci Rep 2017;7:12408.
[25] Li L, Jin G, Jiang J, Zheng M, Jin Y, Lin Z, Li G, Choi Y, Yan G. Cornuside inhibits mast cell-mediated allergic response by down-regulating MAPK and NF-κB signaling pathways. Biochem Biophys Res Commun 2016;473:408–14.
[26] Ge G, Yan Y, Cai H. Ginsenoside Rh2 inhibited proliferation by inducing ROS mediated ER stress dependent apoptosis in lung cancer cells. Biol Pharm Bull 2017;40:2117–24.
[27] Kim JH, Yi YS, Kim MY, Cho JY. Role of ginsenosides, the main active components of Panax ginseng, in inflammatory responses and diseases. J Ginseng Res 2017;41:435–43.
[28] Li Q, Li Y, Wang X, Fang X, He K, Guo X, Zhan Z, Sun C, Jin YH. Co-treatment with ginsenoside Rh2 and betulinic acid synergistically induces apoptosis in human cancer cells in association with enhanced capsase-8 activation, bax translocation, and cytochrome c release. Mol Carcinog 2011;50:760–9.
[29] Lodhi RS, Nakabayashi K, Suzuki K, Yamada AY, Hazama R, Ebina Y, Yamada H. Relaxin has anti-apoptotic effects on human trophoblast-derived HTR-8/SV neo cells. Gynecol Endocrinol 2013;29:1051–64.
[30] Khassawneh B, Tsai SC, Meltzer LJ. Polysomnographic characteristics of adolescents with asthma and low risk for sleep-disordered breathing. Sleep Breath 2019;23:943–51.
[31] Shou Q, Lang J, Jin L, Fang M, Cao B, Cai Y, Ni Z, Qiu F, Li C, Cao G, et al. Total glucosides of peony improve ovalbumin-induced allergic asthma by inhibiting mast cell degranulation. J Ethnopharmacol 2019;244:112136.
[32] She NN, Hou Y, Wang YH, Gui Y, Xi GH, Chen XW, Chen KB, Ma CX, Liu XH, Zhang XB. [Effects of 18β-sodium glycyrrhetinic acid on TNF-α expression in rats with allergic rhinitis]. Lin Chung Er Bi Yan Hou Tou Jing Wai Ke Za Zhi 2019;33:262–76.
[33] Li Y, Mu Z, Wang H, Liu J, Jiang F. The role of particulate matters on methylation of IFN-γ and IL-4 promoter genes in pediatric allergic rhinitis. Oncotarget 2018;9:17406–19.
[34] Xiao P, Long X, Zhang L, Ye Y, Guo J, Liu P, Zhang R, Ning J, Yu W, Wei F, et al. Neurotensin/IL-8 pathway orchestrates local inflammatory response and tumor invasion by inducing M2 polarization of Tumor-Associated macrophages and epithelial-mesenchymal transition of hepatocellular carcinoma cells. OncoImmunology 2018;7:1440166.
[35] Shiratori T, Kyumoto-Nakamura Y, Kukita A, Uehara N, Zhang J, Koda K, Kamiya M, Badawy T, Tomoda E, Xu X, et al. IL-1β induces pathologically activated osteoclasts bearing extremely high levels of resorbing activity: a possible pathological subpopulation of osteoclasts, accompanied by suppressed expression of Kindlin-3 and talin-1. J Immunol 2018;200:218–28.
[36] Kim JH, Kim AR, Kim HS, Kim HW, Park YH, You JS, Park YM, Her E, Kim HS, Kim YM, et al. Rhamnus davurica leaf extract inhibits Fyn activation by antigen in mast cells for anti-allergic activity. BMC Compl Alternative Med 2015;15:80.
[37] Jin Y, Zhu M, Guo Y, Foreman D, Feng F, Duan G, Wu W, Zhang W. Fine particulate matter (PM(2.5)) enhances FcεRI-mediated signaling and mast cell function. Cell Signal 2019;5 7:102–19.
[38] Amin K. The role of mast cells in allergic inflammation. Respir Med 2012;106:204–7.
[39] Im YS, Lee B, Kim EY, Min JH, Song DU, Lim JM, Eom JW, Cho HJ, Sohn Y, Jung HS. Antiallergic effect of gami-hyunggyeyeongyotang on ovalbumin-induced allergic rhinitis in mouse and human mast cells. J Chin Med Assoc 2016;79:185–94.
[40] Jiang W, Hu S, Che D, An H, Liu R. A mast-cell-specific receptor mediates Iopamidol induced immediate IgE-independent anaphylactoid reactions. Int Immunopharm 2019;75:105800.
[41] Che D, Hou Y, Zeng Y, Li C, Zhang Y, Wei D, Hu S, Liu R, An H, Wang Y, et al. Dehydroandrographolide inhibits IgE-mediated anaphylactic reactions via calcium signaling pathway. Toxicol Appl Pharmacol 2019;366:46–53.
[42] Shi P, Zhang L, Wang J, Lu D, Li Y, Ren J, Shen M, Zhang L, Huang J. Porcine FcεRI mediates porcine reproductive and respiratory syndrome virus multiplication and regulates the inflammatory reaction. Virol Sin 2018;33:249–60.
[43] Nunes de Miranda SM, Wilhelm T, Huber M, Zorn CN. Differential Lyn-dependence of the SHIP1-deficient mast cell phenotype. Cell Commun Signal 2016;14:12.
[44] Conti P, Shaik-Dasthagirisaheb YB. Mast cell serotonin immunoregulatory effects impacting on neuronal function: implications for neurodegenerative and psychiatric disorders. Neurotox Res 2015;28:147–53.
[45] Rivera J, Olivera A. A current understanding of Fc epsilon RI-dependent mast cell activation. Curr Allergy Asthma Rep 2008;8:14–20.
[46] Shamji MH, Durham SR. Mechanisms of allergen immunotherapy for inhaled allergens and predictive biomarkers. J Allergy Clin Immunol 2017;140:1485–98.
[47] Tamura S, Yoshihira K, Kawano T, Murakami N. Inhibitor for FcεRI expression on mast cell from Verbasucum thapsus L. Bioorg Med Chem Lett 2018;28:3342–65.
[48] Zhang YZ, Yao JN, Zhang LF, Wang CF, Zhang XX, Gao B. Effect of NLRC5 on activation and reversion of hepatic stellate cells by regulating the nuclear factor-κB signaling pathway. World J Gastroenterol 2019;25:3044–55.
[49] Xiao Q, Piao R, Wang H, Li C, Song L. Orientin-mediated Nrf2/HO-1 signal alleviates H(2)O(2)-induced oxidative damage via induction of JNK and PI3K/AKT activation. Int J Biol Macromol 2018;118:747–55.
[50] Wang Z, Xiong L, Wang G, Wan W, Zhong C, Zu H. Insulin-like growth factor-1 protects SH-SY5Y cells against β-amyloid-induced apoptosis via the PI3K/Akt-Nrf2 pathway. Exp Gerontol 2017;87:23–32.
[51] Stähli A, Maheen CU, Strauss FJ, Eick S, Sculean A, Gruber R. Caffeic acid phenethyl ester protects against oxidative stress and dampens inflammation via heme oxygenase 1. Int J Oral Sci 2019;11:1418–26.